

See discussions, stats, and author profiles for this publication at: <https://www.researchgate.net/publication/231735658>

Reactions of Enimines with $[\text{Cp}^*\text{RuCl}]_4$: Half-Open Ruthenocene and Related Species Incorporating Heteroatoms

ARTICLE *in* ORGANOMETALLICS · FEBRUARY 1999

Impact Factor: 4.13 · DOI: 10.1021/om980875a

CITATIONS

18

READS

30

3 AUTHORS, INCLUDING:



[M. Angeles Paz-Sandoval](#)

Center for Research and Advanced Studies of...

55 PUBLICATIONS 555 CITATIONS

SEE PROFILE

Reactions of Enimines with [Cp*RuCl]₄: Half-Open Ruthenocene and Related Species Incorporating Heteroatoms

J. Alfredo Gutierrez,[†] Ma. Elena Navarro Clemente, and
M. Angeles Paz-Sandoval^{*,‡}

Department of Chemistry, Centro de Investigacion y de Estudios Avanzados del IPN,
Apartado Postal 14-740, Mexico 07300 D.F., Mexico

Atta M. Arif and Richard D. Ernst^{*,§}

Department of Chemistry, University of Utah, Salt Lake City, Utah 84112-1194

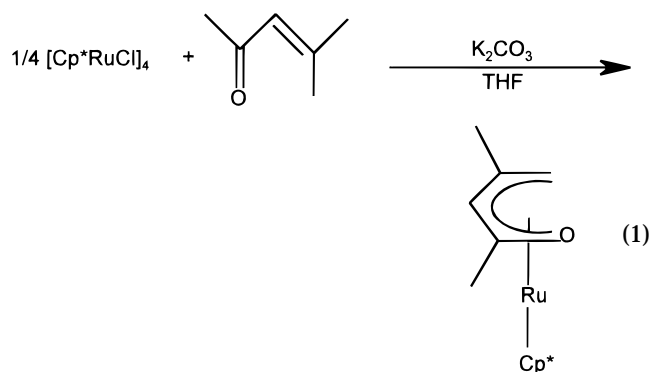
Received October 23, 1998

The reactions of enimines and various silicon, germanium, and tin derivatives with [Cp*RuCl]₄ have been investigated and found to lead to a variety of products, depending on the nature of the enimine and the reaction conditions. In general, mixtures of products were obtained comprised of Cp*Ru(η⁵-azadienyl), Cp*Ru(η³-azadienyl)Cl₂, and Cp*Ru(η⁴-amino-1,3-diene)Cl complexes. Significant differences in both product preferences and overall yields were observed between the silicon, germanium, and tin reagents, the last typically favoring the η⁵ complexes. The choice of solvent also played a major role, the η⁵ complex being slightly to somewhat disfavored in THF relative to benzene. An attempt to convert an η⁴-aminodiene complex, Cp*Ru[η⁴-CH₃CHCHC(CH₃)CHNH(t-Bu)], to an η⁵-azadienyl complex through reaction with Ag⁺ in the presence of K₂CO₃ led to a mixture of species, which included the desired η⁵ complex as well as an unusual Cp*Ru(η³-dienimine)Cl species, which arose from a formal two-electron oxidation followed by two deprotonations, from the nitrogen center and the internal methyl group. Coordination in this species occurs through the nitrogen center and the distal olefin. Structural confirmation for this species, as well as for one η⁴ and three η⁵ complexes, has been obtained.

Introduction

Although simple half-open ruthenocenes utilizing the C₅H₅ ligand are known,¹ it has proven far more convenient to prepare analogues incorporating the C₅Me₅ (Cp*) ligand, due to the availability of the [Cp*RuCl]₄^{2,3} and [Cp*RuCl₂]₂^{4,5} complexes. These complexes can readily be converted to various Cp*Ru(η⁴-diene)Cl,^{2,5} Cp*Ru(η³-C₃H₅)Cl₂,⁴ and functionalized Cp*Ru(η⁵-pentadienyl)^{3,5} complexes in high yield, many of the reactions with [Cp*RuCl₂]₂ undoubtedly proceeding through the intermediacy of [Cp*RuCl]₄.^{2,6} Furthermore, reactions of the tetramer with appropriate enones or enals can be used to prepare some related Cp*Ru(η⁵-oxopentadienyl) complexes,³ such as **1** (eq 1), although for some of the less substituted enals, one observes fragmentation

into CO and other unsaturated species which are then incorporated into the metal complex.⁷



Because of the interesting chemistry displayed by these oxygen-containing molecules, and especially their major differences relative to the simple dienyl complexes, it appeared that the analogous chemistry of nitrogen-containing enimines should also prove interesting. In fact, some η³- or η⁴-azapentadienyl complexes have been previously reported from the reaction of ClIr(PMe₃)₃ with potassium *tert*-butylazapentadienide,⁸ and an η⁵-azapentadienyl complex has been prepared via the

[†] On leave from the Departamento de Posgrado en Quimica, Facultad de Quimica, Universidad de Guanajuato.

[‡] E-mail: mpaz@mail.cinvestav.mx.

[§] E-mail: ernst@chemistry.utah.edu.

(1) (a) Ernst, R. D. *Chem. Rev.* **1988**, *88*, 1255 and references therein. (b) Ernst, R. D. *Struct. Bonding (Berlin)* **1984**, *57*, 1.

(2) Fagan, P. J.; Mahoney, W. S.; Calabrese, J. C.; Williams, I. D. *Organometallics* **1990**, *9*, 1843 and references therein.

(3) Trakarnpruk, W.; Arif, A. M.; Ernst, R. D. *Organometallics* **1992**, *11*, 1686.

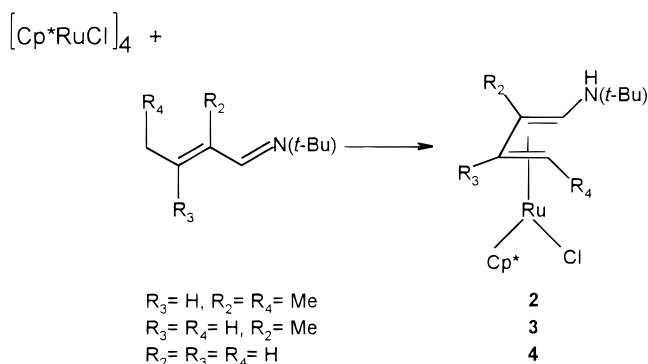
(4) Nagashima, H.; Mukai, K.; Shiota, Y.; Ara, K.-I.; Itoh, K.; Suzuki, H.; Oshima, N.; Moro-oka, Y. *Organometallics* **1985**, *4*, 1314.

(5) Bosch, H. W.; Hund, H. U.; Nietlispach, D.; Salzer, A. *Organometallics* **1992**, *11*, 2087.

(6) Koelle, U.; Kossakowski, J. *J. Organomet. Chem.* **1989**, *362*, 383.

(7) Trakarnpruk, W.; Arif, A. M.; Ernst, R. D. *Organometallics* **1994**, *13*, 2423.

Scheme 1



nucleophilic addition of (t-Bu)NH₂ to the oxopentadienyl complex $[\text{Mn}(\text{CO})_3(\eta^5\text{-CH}_2\text{CHCHCOMe})]$ in the presence of $\text{BF}_3\cdot\text{OEt}_2$.⁹ We have therefore extended our work to ruthenium azadienyl chemistry, which has turned out to have some unique aspects of its own. In this paper we report the preparations of several complexes of the general formulas $\text{Cp}^*\text{Ru}(\eta^4\text{-tert-butyl-1,3-azapentadiene})\text{Cl}$ (**2–5**), $\text{Cp}^*\text{Ru}(\eta^5\text{-tert-butylazapentadienyl})$ (**6–10**), and $\text{Cp}^*\text{Ru}(\eta^3\text{-tert-butyl-[syn-(2,3,4-}\eta)]\text{-azapentadienyl})\text{Cl}_2$ (**11**), as well as a cross-conjugated $\text{Cp}^*\text{Ru}(\eta^3\text{-tert-butylidienimine})\text{Cl}$ complex (**12**). Herein, we report on our observations of this chemistry.

Results and Discussion

As reactions of $[\text{Cp}^*\text{RuCl}]_4$ with 2-methyl-2-pentenal in the presence of K_2CO_3 lead cleanly to the formation of the oxopentadienyl complex $\text{Cp}^*\text{Ru}(\eta^5\text{-CHMeCHCMeCHO})$ (**1**),³ our initial attempts to prepare nitrogen-containing relatives employed the related enamine, in which O was replaced by N(CMe₃). A reaction was indeed observed under similar conditions, but an entirely different course was followed (Scheme 1). First, the chloride was retained in the product, but additionally, an isomerization of the enimine to a cis- η^4 -coordinated diene occurred, yielding complex **2**. The formation of **2** can be expected to be more favorable than that of an η^4 -enimine complex on the basis of previous observations for the Cp^*Ru fragment.³ It is proposed that the expected η^4 -enimine complex is initially formed but at some point the C=N bond decoordinates, and an allylic C–H bond oxidatively adds to ruthenium, after which the hydrogen is transferred to nitrogen, leading to the η^4 -aminodiene species (Scheme 1). The analogous red compounds **3** and **4** were also isolated from a synthetic procedure similar to that used for compound **2**. Compounds **2–4** can also be prepared without K_2CO_3 , while **5** was obtained as a mixture with the corresponding η^5 -azapentadienyl complex **6** from a transmetalation reaction as described in Scheme 2a. The constitutions of the η^4 complexes, which decompose without melting, were verified spectroscopically; the structure of complex **2** was also determined through a single-crystal X-ray diffraction study (vide infra). Complexes **2–5** are thus additional examples of $\text{Cp}^*\text{Ru}(\text{diene})\text{Cl}$ species^{2,5} (Scheme 1).

As the chloride ligand was not removed by K_2CO_3 in refluxing THF, more forcing conditions were sought. Addition of 1 equiv of AgOTf to **2** was found to lead to a new product, **12**, along with the expected η^5 complex **7**, although the yields appeared to be relatively low for both species. Subsequent characterization of **12** through single-crystal X-ray diffraction revealed that once again the chloride ligand had not been lost but, rather, a loss of H_2 from **2** had occurred. Thus, in a formal sense, after a two-electron oxidation, 2 equiv of H^+ was released, yielding **12** (Scheme 3). Notably, the formation of **12** entails the clean elimination of hydrogen atoms from the nitrogen atom as well as the internal methyl group. It could be that this process is initiated by coordination of the first Ag^+ to the lone pair of electrons on the nitrogen center.

A successful synthesis of a nitrogen-containing half-open ruthenocene was ultimately realized from the azadienyl anions or through tin, germanium, and silicon reagents, as described in Schemes 4 and 2a, respectively. Thus, the complex $[\text{Cp}^*\text{RuCl}]_4$ reacts readily with lithium *tert*-butylazapentadienide, prepared in situ at -78°C from *tert*-butylazapentadiene and lithium diisopropylamide (LDA) in THF, to yield the corresponding $\text{Cp}^*\text{Ru}(\eta^5\text{-azapentadienyl})$ complexes **7**, **8**, and **10** in high yield (Scheme 4). However, the inverse addition of $[\text{Cp}^*\text{RuCl}]_4$ to the azapentadienide afforded instead $\text{Cp}^*\text{Ru}(\eta^5\text{-azapentadienyl})$ and Cp^*_2Ru in a 1:1 ratio. Therefore, to avoid this, the azapentadienide ion must be added to the tetramer in THF solution.

The group 14 enimine derivatives $\text{Me}_3\text{MCH(R}_4\text{)C(R}_3\text{)C(R}_2\text{)CHN(CMe}_3\text{)}$ ($\text{M} = \text{Si, Ge, Sn}$), were also useful reagents to give, through a transmetalation reaction with the ruthenium tetramer,¹⁰ compounds **6–10**, as well as **4**, **5**, and **11** (Scheme 2a). We found that in the synthesis of **10** a significant proportion of **4** was also present in the crude reaction mixture. The ratio of these products was quite variable, being 55/45 in one case and 80/20 in another, depending on the quality of the $[\text{Cp}^*\text{RuCl}]_4$ used. When at least one methyl substituent was located on either the R_2 or R_3 position of the group 14 enimine derivatives, formations of the η^5 species **7–9** were generally preferred. In contrast, in the absence of any methyl substituents, treatment with $[\text{Cp}^*\text{RuCl}]_4$ afforded a mixture of η^4 -, η^5 -, and η^3 -azapentadienyl ruthenium complexes (**4**, **10**, and **11**, respectively). Perhaps the species without internal methyl groups exist nearly exclusively in all-trans conformations, as is true of the tin precursor¹¹ to compounds **4**, **10**, and **11**, and such geometries do not readily allow for subsequent rearrangements to possible η^4 and η^5 complexes. In contrast, with the presence of some internal methyl substituents, the adoption of cis conformers could be more facile, thereby allowing for hydrogen atom abstraction processes as well as enhanced favorabilities of U-shaped dienyl conformers.

The ratio of the species formed from reactions of $\text{Me}_3\text{-MCH}_2\text{CH=CHCH=N(CMe}_3\text{)}$ ($\text{M} = \text{Si, Ge, Sn}$) complexes and $[\text{Cp}^*\text{RuCl}]_4$ was dependent on the solvent. NMR studies showed that reactions carried out in C_6D_6 and

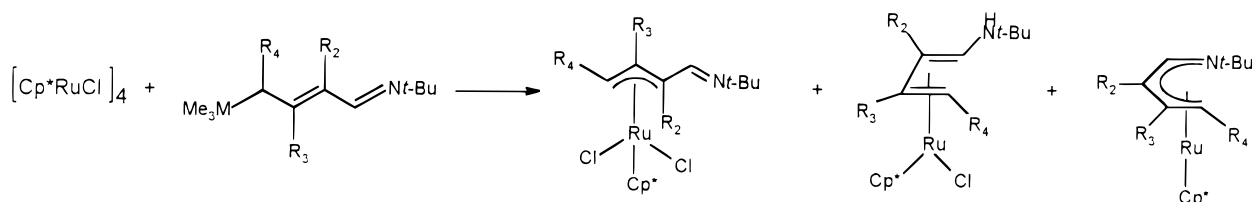
(8) Bleeke, J. R.; Luaders, S. T.; Robinson, K. D. *Organometallics* **1994**, *13*, 1592.

(9) Cheng, M.-H.; Cheng, C.-Y.; Wang, S.-L.; Peng, S.-M.; Liu, R.-S. *Organometallics* **1990**, *9*, 1853.

(10) It is important to mention that the quality of $[\text{Cp}^*\text{RuCl}]_4$ is quite dependent on the $\text{RuCl}_3\cdot\text{H}_2\text{O}$ used and, consequently, the yields of the azapentadienyl complexes prepared from both methods could dramatically change.

(11) Gutierrez, J. A.; Paz-Sandoval, M. A. Unpublished results.

Scheme 2



- a) M = Sn
 $R_2 = R_3 = \text{H}$, $R_4 = \text{Me}$
 $R_3 = \text{H}$, $R_2 = R_4 = \text{Me}$
 $R_3 = R_4 = \text{H}$, $R_2 = \text{Me}$
 $R_2 = R_4 = \text{H}$, $R_3 = \text{Me}$

M = Si, Ge, Sn

$R_2 = R_3 = R_4 = \text{H}$

- b) $R_2 = R_3 = R_4 = \text{H}$

M

THF

C_6D_6

THF

C_6D_6

THF

C_6D_6

Si

89.5

traces

10.5

100

traces

not observed

Ge

7.5

traces

88.7

39.7

3.8

60.3

Sn

traces

traces

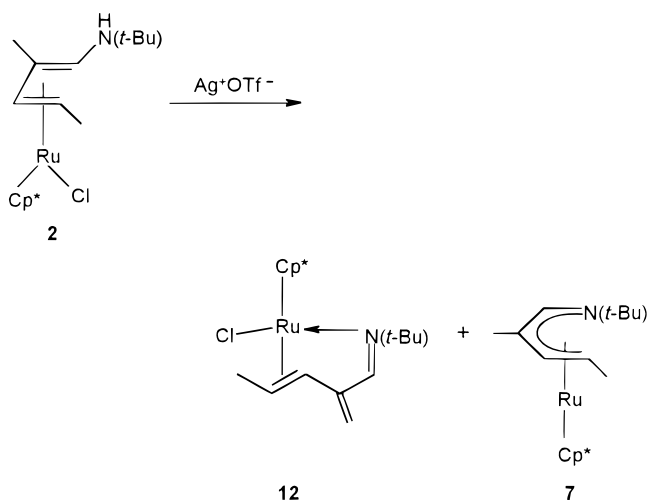
43.5

32.2

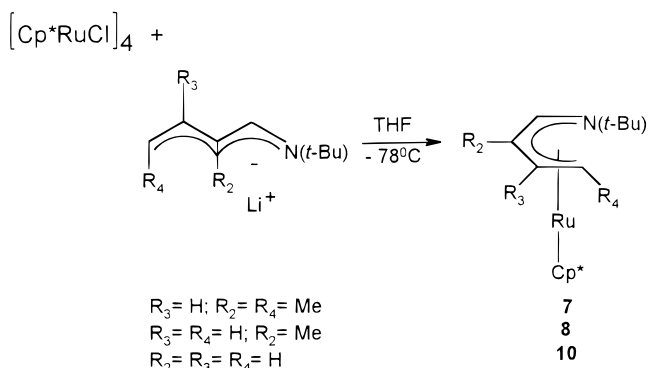
56.5

67.8

Scheme 3



Scheme 4



THF afforded mixtures of products as described in Scheme 2b. Reactions involving the Si derivative tended to favor the formation of an η^3 complex in THF, while

the η^4 complex was formed almost exclusively in C_6D_6 . In comparison, the Ge derivatives led to the formation of η^3 , η^4 , and η^5 complexes, with preferential formation of an η^4 complex in THF, while in C_6D_6 the η^5 complex dominated, followed by the η^4 species, with only traces of the η^3 complex being observed. The formation of the η^3 complex was unexpected for the synthetic route employed, but its formulation was supported by the complete characterization of the analogous oxopentadienyl Ru(IV) complex $[\text{Cp}^*\text{Ru}(\text{Cl})_2(\text{syn-}\eta^3\text{-CH}_2\text{CMeCHC-MeO})]$, formed through formal oxidative addition of chlorine atoms (from CHCl_3) to $\text{Cp}^*\text{Ru}(\eta^5\text{-2,4-dimethyl-oxopentadienyl})$.¹² Similar complexes have also been prepared, such as $\text{Cp}^*\text{Ru}(\text{Cl})_2(\text{syn-}\eta^3\text{-2,4-dimethylpentadienyl})$,¹² $\text{Cp}^*\text{Ru}(\text{Br})_2(\text{syn-}\eta^3\text{-CH}_2\text{CHCHCH}=\text{CHMe})$, and $\text{Cp}^*\text{Ru}(\text{Br})_2(\text{anti-}\eta^3\text{-CH}_2\text{CHCHCHO})$.¹³

In contrast, the Sn derivatives favored formation of an η^5 complex in all cases. However, a higher yield was obtained in C_6D_6 compared to the reaction in THF for the unsubstituted complex 10. This fact may suggest that for Sn derivatives a nonpolar mechanism is favored.

An interesting observation in the transmetalation reactions with unsubstituted Si, Ge, and Sn azapentadiene derivatives was that, in addition to the different ratios of the η^3 , η^4 , and η^5 complexes obtained, some free aminobutadiene, $\text{CH}_2=\text{CHCH}=\text{CHNH}(\text{CMe}_3)$, was always present. This free ligand is an isomerized product of the enamine, formed through protonation of the nitrogen atom, and is present in the η^4 species. To explain how this aminobutadiene could be formed, because of the lack of an obvious source of hydrogen, we investigated not only the possible participation of

(12) Navarro-Clemente, M. E.; Cervantes-Vazquez, M.; Juarez-Saavedra, P.; Paz-Sandoval, M. A. Unpublished results.

(13) Gemel, C.; Mereiter, K.; Schmid, R.; Kirchner, K. *Organometallics* **1996**, *15*, 532.

Table 1. ¹H NMR Data^a for (Azapentadiene)- and (Azapentadienyl)ruthenium Complexes

	H1	H2	H3	H4(anti)	H4(syn)	Cp*	t-Bu	NH
2	4.88 d (4.76) ^d <i>J</i> = 12.84	1.33 s ^b (1.33)	4.16 d (4.11) <i>J</i> = 9.72	2.42 dq (2.26) <i>J</i> = 9.55 <i>J</i> = 6.27 <i>J</i> = 6.24	1.59 d ^c (1.54) <i>J</i> = 6.3	1.39 s (1.37)	1.26 s (1.23)	2.80 d, br (2.79) <i>J</i> = 12.80
3	5.26 d <i>J</i> = 13.2	1.34 s ^b	4.16 dd <i>J</i> = 10.1 <i>J</i> = 7.5	1.96 dd <i>J</i> = 10.1 <i>J</i> = 2.0	2.94 dd <i>J</i> = 7.5 <i>J</i> = 2.0	1.42 s	1.27 s	n.o.
4	5.30 dd <i>J</i> = 13.20 <i>J</i> = 11.20	3.66 dd <i>J</i> = 11.20 <i>J</i> = 5.94	4.0 m	2.12 dd <i>J</i> = 10.56 <i>J</i> = 1.98	3.03 dd <i>J</i> = 7.26 <i>J</i> = 1.98	1.45 s	1.19 s	3.12 d, br <i>J</i> = 13.20
5	4.92 dd <i>J</i> = 12.64 <i>J</i> = 10.90	3.50 dd <i>J</i> = 10.90 <i>J</i> = 5.70	4.03 dd <i>J</i> = 9.65 <i>J</i> = 5.70	2.60 dq <i>J</i> = 9.65 <i>J</i> = 6.18	1.60 d ^c <i>J</i> = 6.18	1.39 s	1.16 s	2.86 d <i>J</i> = 12.37
7	5.95 s	1.74 s ^b	3.69 d <i>J</i> = 9.52	3.36 dq <i>J</i> = 9.52 <i>J</i> = 6.22	1.61 d ^c <i>J</i> = 6.22	1.64 s	1.15 s	
8	6.02 s, br	1.69 s ^b	3.65 ddd <i>J</i> = 10.14 <i>J</i> = 8.41 <i>J</i> = 1.48	2.66 d <i>J</i> = 10.14	2.85 d <i>J</i> = 8.41	1.63 s	1.15 s	
9	6.12 d <i>J</i> = 3.66	4.16 d <i>J</i> = 3.48	1.60 s ^e	2.55 s	2.86 s	1.71 d ^f	1.15 s	
10	6.13 d <i>J</i> = 3.30	4.12 dd <i>J</i> = 5.94 <i>J</i> = 3.30	3.76 m	2.64 d <i>J</i> = 10.56	2.95 d <i>J</i> = 8.58	1.71 s	1.16 s	
11-syn-cis	8.11 d <i>J</i> = 8.41	3.09 dd <i>J</i> = 10.14 <i>J</i> = 8.66	5.62 dt <i>J</i> = 9.90 <i>J</i> = 6.43	1.70 d <i>J</i> = 8.41	4.08 d <i>J</i> = 6.43	1.09 s	1.22 s	
11-syn-trans	8.36 d <i>J</i> = 8.42	2.96 dd <i>J</i> = 9.90 <i>J</i> = 8.48	5.75 dt <i>J</i> = 9.52 <i>J</i> = 6.22	1.76 d <i>J</i> = 9.52	4.19 d <i>J</i> = 6.22	1.12 s	1.28 s	

^a In C₆D₆. δ values are given in ppm and *J* values in hertz. ^b Me (R₂). ^c Me (R₄). ^d Toluene-*d*₈. ^e Me (R₃). ^f Cp* signal shows *J* = 0.13 Hz.

Table 2. ¹³C NMR Data^a for (Azapentadiene)- and (Azapentadienyl)ruthenium Complexes

	C1	C2	C3	C4	R ₂	R ₃	R ₄	Cp*		t-Bu	
								Me	C	Me	C
2^b	105.31 d <i>J</i> = 178.3	80.70 s	88.00 d <i>J</i> = 161.2	62.10 d <i>J</i> = 159.1	18.2 q	30.0 q <i>J</i> = 127.6		9.71 q <i>J</i> = 126.9	88.75 s	29.54 q <i>J</i> = 126.4	52.10 s
4	117.46	72.82	81.03	47.85				9.07	88.43	28.00	51.96
5^c	116.18	70.13	84.35	61.29			17.04	8.70	87.14	28.55	51.25
7	108.91 d <i>J</i> = 157.6	79.23 s	92.76 d <i>J</i> = 144.3	65.68 d <i>J</i> = 165.3	20.06 q <i>J</i> = 123.4		19.24 q <i>J</i> = 127.8	11.04 q <i>J</i> = 125.6	85.55 s	30.70 q <i>J</i> = 125.6	54.55 s
8	109.76	82.94	86.45	53.25	19.10			10.39	88.21	29.96	54.18
9	110.47	76.89	98.64	54.82		25.47		12.62	86.98	31.47	55.58
10	110.53	76.34	87.16	53.86				11.41	86.53	30.51	54.63
11-syn-cis	160.79 (161.06) ^d	77.62 (76.82)	97.20 (100.14)	65.09 (61.68)				8.79	104.61	29.47 (29.93)	53.44 (58.95)
11-syn-trans	160.31	76.66	99.75	60.96				8.76	104.91	29.80	n.o.

^a In C₆D₆. δ values are given in ppm and *J* values in hertz. ^b In toluene-*d*₈. ^c In THF-*d*₈. ^d In CDCl₃.

the THF and C₆D₆ solvents in these reactions but also the reactivity and potential disproportionation reactions of some of the isolated compounds. These studies have allowed us to propose tentative mechanisms (vide infra) which are intended to explain the formation of the new η^3 -, η^4 -, and η^5 -aza(diene, dienyl) ruthenium complexes. It is clear from the comparative study between Si, Ge, and Sn derivatives that the Si complexes react by a completely different mechanism than Ge and Sn. Unfortunately, no intermediate species were isolated and just a few were detected through the ¹H NMR experiments. The ¹H and ¹³C NMR data of the isolated complexes **2–5** and **7–11** are summarized in Tables 1 and 2.

In C₆D₆ the reaction between Me₃GeCH₂CH=CH-CH=N(CMe₃) and [Cp*RuCl]₄ showed clearly the competition between η^4 and η^5 species,¹⁴ the η^5 species being observed in C₆D₆ only in traces at the beginning but as a major component when the reaction finished, while

in THF the η^4 complex predominated, suggesting that an oxidative addition is probably favored in a more polar solvent. The preferential formation of η^5 complexes in C₆D₆ for Ge, as well as for the Sn derivatives (vide supra), suggests a concerted mechanism in which Ru–Cl and Sn–C(σ) bonds are broken, giving Ru–C(π) and Sn–Cl bonds.¹⁵ Consistent with the experimental results, this mechanism is favored in C₆D₆ because uncharged species are formed. The observations concerned with the favorability of formation of η^5 complexes from group 14 reagents in the sequence Sn > Ge > Si correlate well with the expected M–C bond polarity.¹⁶

(14) In the case of the Ge derivative it was also observed that an isomerization of the aminodiene took place, giving the mixture of *Z,E* and *E,E* α,β -unsaturated crotonaldehydes in a 1:1.2 ratio.

(15) (a) Paz-Sandoval, M. A. Ph.D. Thesis, University of London, 1983; p 61. (b) Abel, E. W.; Moorhouse, S. *J. Chem. Soc., Dalton Trans.* **1973**, 1706.

(16) Elschenbroich, Ch.; Salzer, A. *Organometallics*, 2nd ed.; VCH: Weinheim, Germany, 1992; p 94.

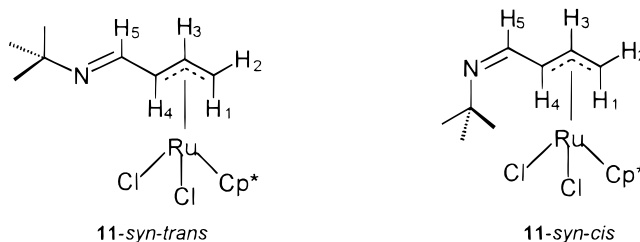
In the reactions with Sn and Ge derivatives, on changing from THF to C_6D_6 solvents, the η^5 complex **10** is favored substantially, going from 56% to 68%, and 4% to 60%, respectively. These results are in agreement with the trend expected from the M–C bond strengths.

The stronger Si–C bond was found to react differently, suggesting that a concerted mechanism¹⁵ was not favored at all. There was a strong preference for the η^3 -Ru(IV) complex **11** in THF, while formation of the η^4 complex **4** was favored in C_6D_6 , as described previously (Scheme 2b). Despite the Si derivative's stronger Si–C bond, no evidence of any organometallic silicon–ruthenium complexes was observed. In C_6D_6 , the reaction with the Si derivative was found to be very slow, requiring 18 h at room temperature, while Sn derivatives only required 1 h. Monitoring the reaction through 1H NMR showed broad signals, which suggested the presence of paramagnetic species. From the beginning there was evidence of the formation of the η^4 complex **4**, along with traces of the η^5 complex **10**, which finally disappeared, giving traces of the η^3 complex **11**. When the reaction had almost finished, the broadening was gone, giving narrow signals again, which revealed that the free aminodiene and the η^4 complex **4** were the major products. If the reaction products remained in solution for longer times, there was complete decomposition to unidentified species. The reaction in THF showed the η^3 complex **11** to be a major product along with the η^4 complex **4** in a 9:1 ratio, respectively.

The η^3 complex **11** and the silicon derivative $Me_3SiCH_2CH=CHCH=N(CMe_3)$ were observed in a 1:1.2 ratio, respectively, suggesting that some $[Cp^*RuCl]_4$ reacts by another pathway, which is in accord with the evidence by 1H NMR of Me_3Si signals at high field (0.1–0.31 and 0.8–1.8 ppm). This suggests a nonconcerted mechanism, in which the formation of Me_3SiCl perhaps allows for the generation of the coordinatively unsaturated complex $Cp^*Ru(\eta^3\text{-azapentadienyl})(Cl)$, and this $17e^-$ species then reacts again in the presence of Me_3SiCl to give the corresponding Ru(IV) complex **11**, along with the dimer $Me_3SiSiMe_3$. Oxidative additions from electrophilic fragments have been reported to be complicated, and single-electron transfer represents a viable alternative.¹⁷ As another alternative, one can consider the possible formation of a $Cp^*Ru(THF)_2Cl$ complex, which may react with azapentadienide or a free aminobutadiene, thereby yielding the η^3 and η^4 complexes **11** and **4**.

The isolated product **10**, upon dissolution in $CDCl_3$ and examination by 1H NMR spectroscopy, showed after 15 min resonances due to complexes **4** and **11**. Complex **11** was observed as a mixture of two syn η^3 isomers, which have a *tert*-butyl group in the *cis* or *trans* position (Chart 1). The **11-syn-cis**:**11-syn-trans**:**4** ratio was 6:1:1, respectively. Addition of 2 drops of $CHCl_3$ to an NMR tube containing compound **10** in C_6D_6 led, after 45 min, to the presence of compounds **11-syn-cis**, **11-syn-trans**, and **4**, in the ratio previously mentioned. Upon standing at room temperature for 20 h, complex **10** was completely consumed, giving the three species **11-syn-cis**, **11-syn-trans**, and **4**. In contrast, if compound **10** (85 mg)

Chart 1



was stirred for 15 h at room temperature in 20 mL of C_6H_6 in the presence of a stoichiometric amount of $CHCl_3$ (18.91 μ L), a mixture of **11-syn-cis**, **11-syn-trans**, **4**, and **10** was observed in a 4:1:1:1 ratio (see Experimental Section).

Subsequent NMR spectroscopic examination of the reaction mixture revealed that the **11-syn-cis** compound underwent slow isomerization to the **11-syn-trans** isomer. This result, along with those discussed above, suggests that **11-syn-cis** is the kinetic isomer and **11-syn-trans** the thermodynamic one.

To understand the interconversion between the η^3 , η^4 , and η^5 species, a pure sample of the η^4 -azapentadiene complex **4** in C_6D_6 was studied through 1H NMR. After 6 h, approximately 30% of the starting material **4** was already converted to the η^5 -azapentadienyl complex **10** and the η^3 -azapentadienyl species **11-syn-cis** in a 1:1 ratio. The latter complex after 4 days at room temperature was transformed completely to the **11-syn-trans** complex.

We observed that compound **11** reacted further in solution; however, we were not able to fully characterize any products, neither from the reaction of **10** in $CHCl_3$ nor from the reaction of **4** in C_6H_6 . Comparatively, both compounds **10** and **11** are much more stable in C_6D_6 , while **4** disproportionates to compounds **10** and **11**. Finally, these three azapentadienyl compounds **4**, **10**, and **11** are prone to react with $CHCl_3$. Attempts to crystallize compound **11** led to decomposition. The apparent instability of **11** contrasts with the analogous $Cp^*Ru(\eta^3\text{-pentadienyl})(Cl)_2$ and $Cp^*Ru(\eta^3\text{-oxopentadienyl})(Cl)_2$ complexes, which are much more stable. The reason could be steric in origin due to unfavorable interactions between the *t*-Bu group of the azapentadienyl ligand and the Cp^* and chloride ligands. However, we cannot discriminate between this and the possibility that impurities, which are always present in the reaction mixture, could be the major problem. It is known that the electrophilic " Cp^*Ru^+ " fragment¹⁸ induces activation of C–Cl bonds easily, with the corresponding formation of several " Cp^*RuCl " clusters which could compete with the formation of $Cp^*Ru(\eta^3\text{-azapentadienyl})(Cl)_2$ complex **11**.

Structural Studies. Crystal data for compounds **2**, **7**, **8**, **10**, and **12** are provided in Table 3. The structure of the η^4 -diene complex **2** is presented in Figure 1 and is generally similar to those of related species.^{2,19} Some

(17) Collman, J. P.; Hegedus, L. S.; Norton, J. R.; Finke, R. G. *Principles and Applications of Organotransition Metal Chemistry*; University Science Books: Mill Valley, CA, 1987; p 308.

(18) (a) Carreno, R.; Urbanos, F.; Dahan, F.; Chaudret, B. *New J. Chem.* **1994**, 18, 449 and references therein. (b) Chaudret, B. *Bull. Soc. Chim. Fr.* **1995**, 132, 268. (c) Rondon, D.; Delbeau, J.; He, X.-D.; Sabo-Etienne, S.; Chaudret, B. *J. Chem. Soc., Dalton Trans.* **1994**, 1895 and references therein.

(19) (a) Freeman, W. P.; Tilley, T. D.; Rheingold, A. L.; Ostrander, R. L. *Angew. Chem., Int. Ed. Engl.* **1993**, 32, 1744. (b) Hughes, R. P.; Rose, P. R.; Zheng, X.; Rheingold, A. L. *Organometallics* **1995**, 14, 2407.

Table 3. Crystal Data for 2, 7, 8, 10, and 12

	$\text{C}_{20}\text{H}_{34}\text{NClRu}$ (2)	$\text{C}_{20}\text{H}_{33}\text{NRu}$ (7)	$\text{C}_{19}\text{H}_{31}\text{NRu}$ (8)	$\text{C}_{18}\text{H}_{29}\text{NRu}$ (10)	$\text{C}_{20}\text{H}_{32}\text{NClRu}$ (12)
mol wt	425.024	388.56	374.53	360.49	423.008
cryst syst	<i>Fdd2</i>	<i>P2₁/c</i>	<i>P1</i>	<i>C2/c</i>	<i>P2₁/n</i>
<i>a</i> (Å)	26.365(8)	9.256(2)	9.3099(8)	13.574(6)	9.159(3)
<i>b</i> (Å)	41.604(9)	19.435(4)	12.400(3)	11.199(4)	15.795(5)
<i>c</i> (Å)	7.687(2)	11.200(3)	16.614(5)	23.607(6)	13.949(4)
α (deg)	90	90	83.42(3)	90	90
β (deg)	90	105.66	74.47(1)	97.23(3)	93.43(2)
γ (deg)	90	90	85.22(1)	90	90
<i>V</i> (Å ³)	8431.69	1940.2 (8)	1832.9(7)	3560	2014.18
<i>Z</i>	16	4	4	8	4
cryst size (mm)	$0.37 \times 0.31 \times 0.12$	$0.22 \times 0.19 \times 0.17$	$0.22 \times 0.17 \times 0.17$	$0.25 \times 0.20 \times 0.15$	$0.27 \times 0.25 \times 0.19$
λ (Mo K α) (cm ⁻¹)	0.7107	0.7107	0.7107	0.7107	0.7107
<i>D</i> _{calcd} (g cm ⁻³)	1.339	1.33	1.35	1.345	1.395
scan type	$\theta/2$	$\theta/2$	$\theta/2$	$\theta/2$	$\theta/2$
θ limit (deg)	2–25	0–21	0–23	2–24	2–24
total no. of data	3523	2681	5293	2915	3517
total no. of unique data	3523	1889	4540	2784	3156
total no. of obsd data, (F_o) ² > 3 σ (F_o) ²	1734	1517	3501	2746	2490
decay (%)	0	1.58	3.8	0	0
abs cor range	0.78–1.00	1.16–1.36	0.99–1.21	0.77–0.99	0.96–0.99
final R1	0.0310	0.0371	0.0400	0.0734	0.0296
final wR2	0.0389	0.0415	0.0456	0.1926	0.0393
no. of variables	207	199	412	182	228

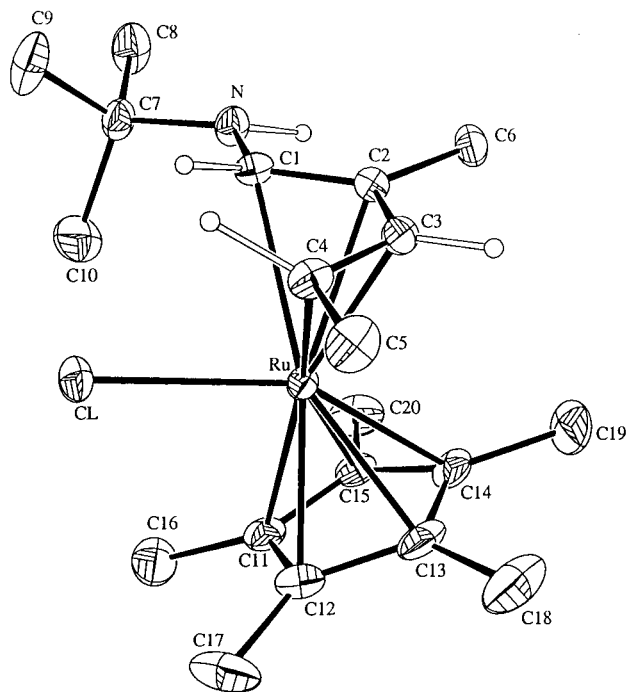


Figure 1. ORTEP drawing of compound 2.

relevant data are provided in Table 4. As in $\text{M}(\text{C}_5\text{R}_5)$ -(pentadienyl)(L) complexes,²⁰ the Ru–Cl vector is nearly parallel with the open (diene) ligand plane but is significantly tilted relative to the C_5R_5 plane.²⁰ A tilt of $20.2(4)^\circ$ results between the two ligand planes. The structure may then be considered to be a hybrid between $\text{M}(\text{diene})_2\text{L}$ (I)²¹ and $\text{M}(\text{C}_5\text{R}_5)_2\text{L}$ (II)²² complexes (Chart 2).

(20) Hyla-Kryspin, I.; Waldman, T. E.; Melendez, E.; Trakarnpruk, W.; Arif, A. M.; Ziegler, M. L.; Ernst, R. D.; Gleiter, R. *Organometallics* **1995**, *14*, 5030.

(21) (a) Huttner, G.; Neugebauer, D.; Razavi, A. *Angew. Chem., Int. Ed. Engl.* **1975**, *14*, 352. (b) Krueger, C.; Tsay, Y.-H. *Angew. Chem., Int. Ed. Engl.* **1971**, *10*, 261. (c) Koerner, von Gustorf, E.; Jaenicke, O.; Polansky, O. E. *Angew. Chem., Int. Ed. Engl.* **1972**, *11*, 532.

(22) (a) Fieselmann, B. F.; Stucky, G. D. *J. Organomet. Chem.* **1977**, *137*, 43. (b) Lauher, J. W.; Hoffmann, R. *J. Am. Chem. Soc.* **1976**, *98*, 1729.

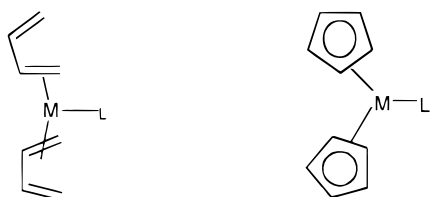
Table 4. Selected Bond Distances (Å) and Angles (deg) for Complex 2^a

Bond Distances			
Ru–Cl	2.476(2)	C3–C4	1.39(1)
Ru–C1	2.500(6)	C4–C5	1.50(1)
Ru–C2	2.300(6)	C7–C8	1.50(1)
Ru–C3	2.154(7)	C7–C9	1.51(1)
Ru–C4	2.251(7)	C7–C10	1.54(1)
Ru–C11	2.212(8)	C11–C12	1.46(1)
Ru–C12	2.158(7)	C11–C15	1.39(1)
Ru–C13	2.154(7)	C11–C16	1.50(1)
Ru–C14	2.186(7)	C12–C13	1.41(1)
Ru–C15	2.218(7)	C12–C17	1.51(1)
N–C1	1.379(8)	C13–C14	1.44(1)
N–C7	1.467(8)	C13–C18	1.51(1)
C1–C2	1.387(9)	C14–C15	1.41(1)
C2–C3	1.438(9)	C14–C19	1.49(1)
C2–C6	1.507(9)	C15–C20	1.51(1)
Bond Angles			
Cl–N–C7	123.7(5)	C12–C11–C16	124.8(8)
N–C1–C2	121.4(6)	C15–C11–C16	127.1(8)
C1–C2–C3	120.2(6)	C11–C12–C13	106.6(7)
C1–C2–C6	120.7(6)	C11–C12–C17	126.7(8)
C3–C2–C6	119.0(6)	C13–C12–C17	126.3(9)
C2–C3–C4	126.1(6)	C12–C13–C14	108.5(7)
N–C7–C8	107.2(6)	C12–C13–C18	125.9(9)
C3–C4–C5	121.2(6)	C14–C13–C18	124.9(9)
N–C7–C9	109.6(7)	C13–C14–C15	107.1(7)
N–C7–C10	110.3(6)	C13–C14–C19	125.0(8)
C8–C7–C9	109.6(7)	C15–C14–C19	126.8(9)
C8–C7–C10	111.2(8)	C11–C15–C14	109.7(7)
C9–C7–C10	108.9(7)	C11–C15–C20	126.5(7)
C12–C11–C15	108.0(6)	C14–C15–C20	123.7(8)

^a Numbers in parentheses in this and all following tables are estimated standard deviations in the least significant digits.

On the basis of data for other diene- and dienylnmetal complexes, significant tilts of most of the diene substituents (N, C5, C6, H3) toward the ruthenium atom would be expected.^{1b} However, each of these at most barely deviates from this plane, perhaps due in part to steric opposition by the Cp* ligand. In contrast, the expected significant tilts by H2 and H4 (whose positions were successfully refined) away from the ruthenium atom are observed, $19(1)^\circ$ and $36(1)^\circ$, respectively, as judged by torsion angles. While the latter value appears reasonable, the substantially smaller tilt by H2 might at first

Chart 2



appear to be cause for concern. However, the Ru–diene bonding is unexpectedly asymmetric, with much longer Ru–C(1 and 2) distances relative to C(4 and 3), 2.500(6) and 2.300(6) Å vs 2.251(7) and 2.154(7) Å. Given the apparently significantly weaker bonding by the C1–C2 double bond, it is reasonable that the degree of substituent tilting would not be so extensive. The origin of the unsymmetric diene coordination would appear to be the greater steric encumbrance brought about by the N and C7 substituents, and support for this can be obtained from the relative deviations by the methyl groups from the cyclopentadienyl plane. Thus, while C18 and C19 tilt out of the C₅ plane away from Ru by 0.22 Å each, the tilt for C20 is only 0.04 Å. The tilts of 0.09 Å each by C16 and C17 also appear reduced, clearly a result of their proximity to Cl. The relevant Ru–C and C–C distances indicate the diene is coordinated as such, rather than as an enediyl. Comparatively, the Cp*–Ru bond lengths were found to be more symmetric relative to the corresponding values in Cp*Ru(η^5 -azapentadienyl) compounds **7**, **8** and **10** (vide infra), while the Ru–aminodiene distances are significantly longer than those of Cp*Ru(η^4 -1,3-butadiene)X (X = OSO₂CF₃,²³ I²) complexes.

The solid-state structures of the half-open azapentadienyl ruthenium complexes **7**, **8**, and **10** are the first examples reported,^{8,9} and their structures are presented in Figures 2–4 respectively, while various bonding parameters are contained in Tables 5–7. The structural parameters for **7**, **8**, and **10** correspond in general fairly closely to each other, with the substituted azapentadienyl complexes **7** and **8** showing the most similar and ordered structures. In the case of structure **8**, there are two crystallographically independent molecules, whose structural parameters are essentially identical. It can be seen that the methyl-substituted complexes **7** and **8** adopt an eclipsed structural pattern, as had been observed as well for various penta-^{24,25} and oxopentadienyl³ analogues, in contrast with Cp*Ru(η^5 -3-C₆H₉).³

As expected, the metal–carbon bonding for these unsymmetrical azapentadienyl complexes **7**, **8**, and **10** is not as regular as found in other half-open ruthenocenes.³ The Ru–C bond distances for the acyclic and cyclic ligands in **7**, **8**, and **10** are quite similar (**7**, 2.192, 2.178 Å; **8**, 2.185, 2.189 Å; **10**, 2.170, 2.169 Å), as was found for the oxopentadienyl analogue Cp*Ru(η^5 -3,5-Me₂C₄H₃O) (**1**; 2.167, 2.168 Å, respectively)³ and the bulky Cp*Ru(η^5 -dimethylnopadienyl) complex (2.196, 2.209 Å, respectively).⁵ One can observe that the methyl-substituted carbon atoms of the azapentadienyl ligands

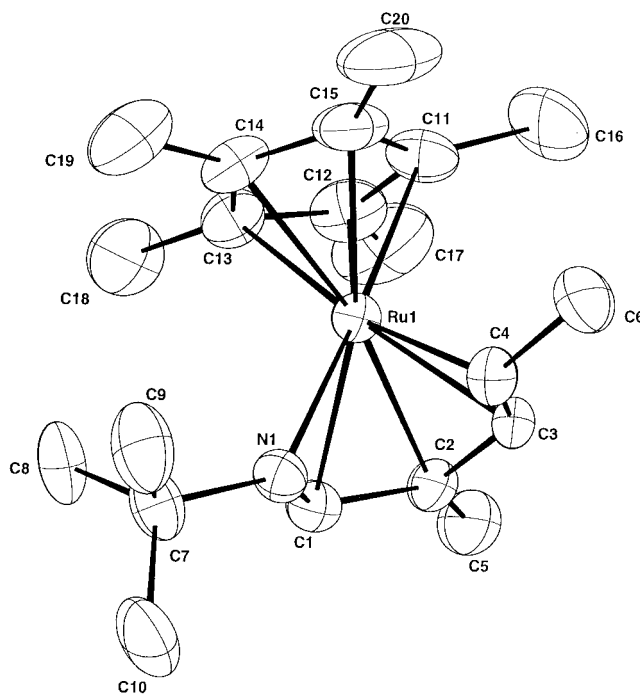


Figure 2. ORTEP drawing of compound **7**.

were characterized by the longest Ru–C(azapentadienyl) distances.

The shortness of the Ru–C(Cp*) bonds in **10** (2.169 Å) could easily be a consequence of the apparently weaker bonding of the azapentadienyl ligand relative to the pentadienyl analogue Cp*Ru(η^5 -3-C₆H₉) (2.19 Å).³ A similar observation has been made for the corresponding oxopentadienyl complex **1** (vide supra). Although the Ru–C(Cp*) bonds are fairly unsymmetric, one can probably gauge the relative strengths of the bonds by the Ru–Cp* plane separations. These vary regularly from 1.834 Å for the 3-C₆H₉ complex to 1.816 for **10** to 1.795 Å for the oxodienyl species, suggesting an enhancement of the RuCp* bonding, with accompanying weakening of the M–PdI bonding, as the pentadienyl ligand becomes more electronegative. The Ru–N bond lengths in **7**, **8**, and **10** range from 2.24 to 2.25 Å, and it is interesting to observe that the corresponding Ru–C(Cp*) bonds “almost trans” to them showed the shortest bond in each case (N–Ru–C(Cp*) and Ru–C(Cp*): 173.5(4)° and 2.138(9) Å (**7**); 172.3(3)° and 2.138(9) Å (**8**); 170.8(7)° and 2.12(2) Å (**10**)), reflecting the steric hindrance of the t-Bu group substituent on the nitrogen atom and the trans effect, since Ru–N bonding appears weaker than the Ru–C bonding.³

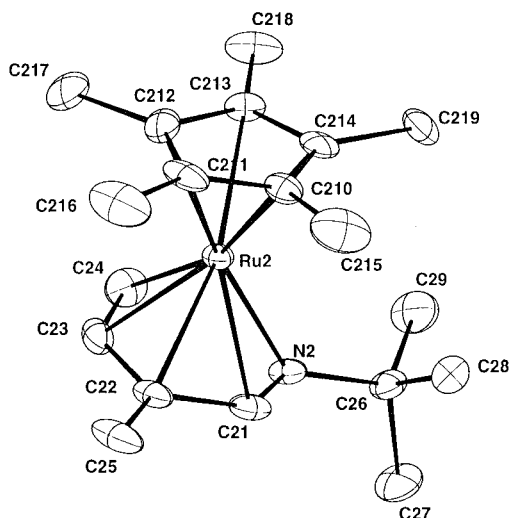
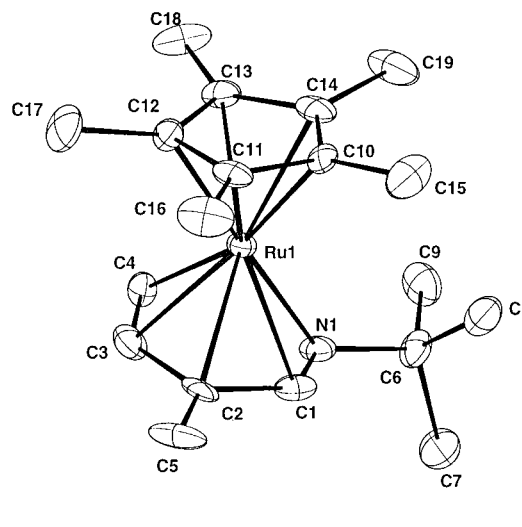
Examination of the backbone C–C–C angles reveals the azadienyl ligands to be similar in girth to the oxodienyl ligand in complex **1** but smaller than the corresponding dienyl ligand in Cp*Ru(η^5 -3-C₆H₉). A comparison between the azadienyl complex **7** and the analogous oxodienyl complex **1** suggests that in these species there is a shortening of the C–CH₃ distances for the terminal vs internal methyl groups (1.482(11) vs 1.530(15) Å and 1.488(12) vs 1.500(12) Å, respectively). The Ru–C(Me_{terminal}) bond is significantly longer in **7** than in **1**, 2.242(8) vs 2.178(7) Å.

The structures for **7** and **8** showed that their azapentadienyls' external N–C and C–C bonds (**7**, 1.341(10), 1.394(11) Å; **8**, 1.33(1), 1.38(1) Å) are clearly

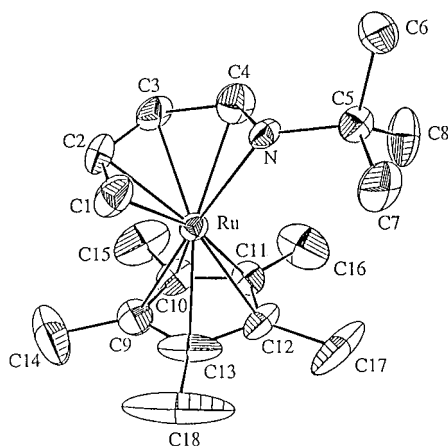
(23) Gemel, C.; Kalt, D.; Mereiter, K.; Sapunov, V. N.; Schmid, R.; Kirchner, K. *Organometallics* **1997**, *16*, 427.

(24) Shen, J. K.; Freeman, J. W.; Hallinan, N. C.; Rheingold, A. L.; Arif, A. M.; Ernst, R. D.; Basolo, F. *Organometallics* **1992**, *11*, 3215.

(25) Gleiter, R.; Hyla-Kryspin, I.; Ziegler, M. L.; Sergenson, G.; Green, J. C.; Stahl, L.; Ernst, R. D. *Organometallics* **1989**, *8*, 298.

Figure 3. ORTEP drawing of compound **8**.Table 6. Selected Bond Distances (Å) and Angles (deg) for Complex **8**

Bond Distances			
Ru1–N1	2.240(6)	Ru1–C1	2.194(7)
Ru1–C2	2.187(7)	Ru1–C3	2.161(8)
Ru1–C4	2.199(9)	Ru1–C10	2.211(7)
Ru1–C11	2.166(7)	Ru1–C12	2.138(7)
Ru2–C13	2.197(7)	Ru1–C14	2.236(7)
Ru2–N2	2.238(6)	Ru2–C21	2.209(7)
Ru2–C22	2.198(7)	Ru2–C23	2.144(8)
Ru2–C24	2.185(8)	Ru2–C210	2.211(8)
Ru2–C211	2.155(7)	Ru2–C212	2.133(7)
Ru2–C213	2.196(7)	Ru2–C214	2.246(7)
N1–C1	1.33(1)	N1–C6	1.48(1)
N2–C21	1.34(1)	N2–C26	1.48(1)
C1–C2	1.44(1)	C2–C3	1.42(1)
C2–C5	1.50(1)	C3–C4	1.38(1)
C6–C7	1.54(1)	C6–C8	1.51(1)
C6–C9	1.52(1)	C10–C11	1.40(1)
C10–C14	1.43(1)	C10–C15	1.49(1)
C11–C12	1.44(1)	C11–C16	1.49(1)
C12–C13	1.43(1)	C12–C17	1.51(1)
C13–C14	1.42(1)	C13–C18	1.49(1)
C14–C19	1.49(1)	C21–C22	1.45(1)
C22–C23	1.40(1)	C22–C25	1.50(1)
C23–C24	1.39(1)	C26–C27	1.53(1)
C26–C28	1.51(1)	C26–C29	1.52(1)
C210–C211	1.42(1)	C210–C214	1.41(1)
C210–C215	1.49(1)	C211–C212	1.42(1)
C211–C216	1.51(1)	C212–C213	1.43(1)
C212–C217	1.50(1)	C213–C214	1.41(1)
C213–C218	1.50(1)	C214–C219	1.50(1)

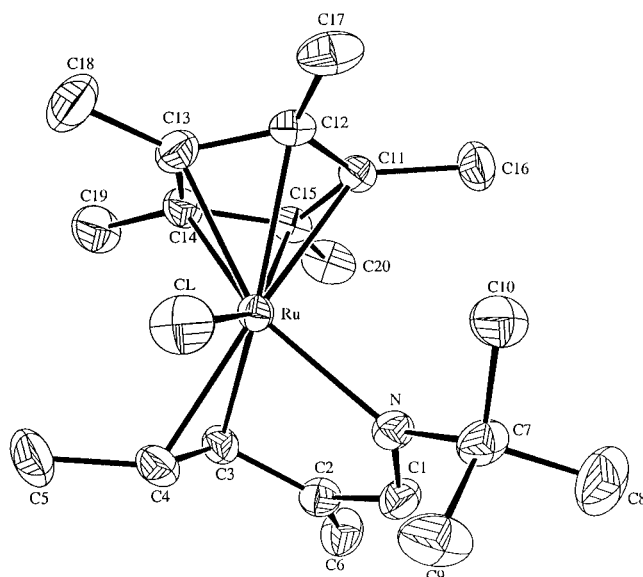
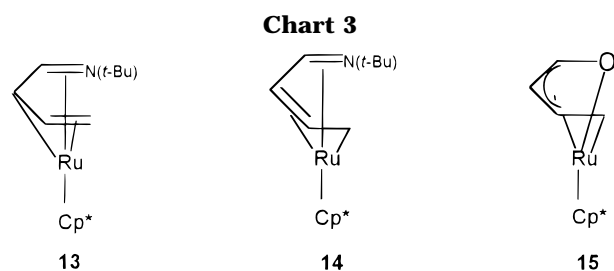
Figure 4. ORTEP drawing of compound **10**.Table 5. Selected Bond Distances (Å) and Angles (deg) for Complex **7**

Bond Distances			
Ru1–N1	2.250(6)	Ru1–C1	2.193(8)
Ru1–C2	2.178(8)	Ru1–C3	2.153(7)
Ru1–C4	2.242(8)	Ru1–C11	2.189(8)
Ru1–C12	2.216(8)	Ru1–C13	2.192(8)
Ru1–C14	2.155(9)	Ru1–C15	2.138(9)
C1–N1	1.341(10)	C1–C2	1.422(10)
C2–C3	1.425(11)	C2–C5	1.488(12)
C3–C4	1.394(11)	C4–C6	1.482(11)
C7–C8	1.513(12)	C7–C9	1.498(13)
C7–C10	1.502(13)	C7–N1	1.492(10)
C11–C12	1.406(12)	C11–C15	1.424(14)
C11–C16	1.487(14)	C12–C13	1.406(12)
C12–C17	1.505(13)	C13–C14	1.410(12)
C13–C18	1.491(12)	C14–C15	1.408(13)
C14–C19	1.470(14)	C15–C20	1.491(14)

Bond Angles			
C1–C2–C3	120.3(7)	C3–C2–C5	120.3(7)
C1–C2–C5	119.2(7)	C3–C4–C6	119.5(7)
C2–C3–C4	128.3(7)	C8–C7–C10	109.3(8)
C8–C7–C9	110.6(8)	C8–C7–N1	114.5(7)
C9–C7–C10	110.1(8)	C10–C7–N1	106.8(7)
C9–C7–N1	105.4(7)	C2–C1–N1	119.3(7)
C1–N1–C7	117.5(7)		

shorter than the internal ones (**7**, 1.425(11), 1.422(10) Å; **8**, 1.44(1), 1.42(1) Å), pointing to a contribution from resonance hybrid **13**, while the unsubstituted structure for **10** is more consistent with a contribution from resonance hybrid **14**, as observed from the correspond-

ing external (N–C 1.33(2) Å, C–C 1.40(2) Å) and internal C–C bond distances (1.36(2), 1.44(2) Å). The alternations in the ligand frameworks contrast with what has been observed for the oxodienyl ligand, in

**Figure 5.** ORTEP drawing of compound **12**.**Table 7. Bond Distances (Å) and Bond Angles (deg) for Complex 10**

Bond Distances			
Ru–N	2.247(10)	Ru–C4	2.21(2)
Ru–C3	2.16(2)	Ru–C2	2.13(2)
Ru–C1	2.18(2)	Ru–C9	2.12(2)
Ru–C10	2.130(14)	Ru–C11	2.223(14)
Ru–C12	2.212(14)	Ru–C13	2.16(2)
N–C4	1.33(2)	N–C5	1.48(2)
C1–C2	1.40(2)	C2–C3	1.36(2)
C3–C4	1.44(2)	C5–C7	1.53(2)
C5–C8	1.53(2)	C5–C6	1.55(2)
C9–C10	1.36(2)	C9–C13	1.43(3)
C9–C14	1.51(2)	C10–C11	1.35(2)
C10–C15	1.56(2)	C11–C12	1.41(2)
C11–C16	1.50(2)	C12–C13	1.40(3)
C12–C17	1.49(2)	C13–C18	1.54(2)
Bond Angles			
C3–C2–C1	126(2)	C2–C3–C4	120(2)
C7–C5–C8	111(2)	C7–C5–C6	108.1(13)
C8–C5–C6	109.9(14)	C10–C9–C13	106(2)
C10–C9–C14	129(2)	C13–C9–C14	129(2)
C11–C10–C9	113(2)	C11–C10–C15	123(2)
C9–C10–C15	124(2)	C10–C11–C12	106(2)
C10–C11–C16	126(2)	C12–C11–C16	127(2)
C13–C12–C11	109(2)	C13–C12–C17	125(2)
C11–C12–C17	125(2)	C12–C13–C9	106.8(14)
C12–C13–C18	124(3)	C9–C13–C18	130(3)

which the participation of resonance hybrid **15** suggests some contribution of a Ru(IV) complex³ (Chart 3).

The structure of the dienimine complex **12** is provided in Figure 5, while important bond lengths and angles are reported in Table 8. All hydrogen atoms on C1, C3, C4, and C6 could be located and refined and were found to occupy the positions expected on the basis of the formal hybridizations of their attached carbon atoms. With a loss of one hydrogen atom from both N and C6,

Table 8. Selected Bond Distances (Å) and Angles (deg) for Complex 12

Bond Distances			
Ru–Cl	2.447(1)	C4–C5	1.506(7)
Ru–N	2.178(3)	C7–C8	1.536(7)
Ru–C3	2.163(4)	C7–C9	1.502(7)
Ru–C4	2.176(4)	C7–C10	1.506(6)
Ru–C11	2.275(4)	C11–C12	1.396(5)
Ru–C12	2.245(4)	C11–C15	1.421(5)
Ru–C13	2.171(4)	C11–C16	1.491(5)
Ru–C14	2.180(4)	C12–C13	1.462(6)
Ru–C15	2.186(4)	C12–C17	1.497(6)
N–C1	1.274(5)	C13–C14	1.408(6)
N–C7	1.517(5)	C13–C18	1.492(7)
C1–C2	1.461(6)	C14–C15	1.439(6)
C2–C3	1.468(6)	C14–C19	1.492(6)
C2–C6	1.307(6)	C15–C20	1.499(6)
C3–C4	1.395(6)		
Bond Angles			
Cl–Ru–N	90.72(9)	N–C7–C9	106.6(4)
Cl–Ru–C3	118.0(1)	N–C7–C10	109.8(3)
Cl–Ru–C4	81.0(1)	C8–C7–C9	110.3(4)
N–Ru–C3	77.8(1)	C8–C7–C10	108.4(4)
N–Ru–C4	82.9(2)	C9–C7–C10	109.4(4)
C3–Ru–C4	37.5(2)	C12–C11–C15	109.1(3)
Ru–N–C1	112.6(3)	C12–C11–C16	126.8(4)
Ru–N–C7	130.4(3)	C15–C11–C16	124.1(4)
C1–N–C7	117.0(3)	C11–C12–C13	107.0(3)
N–C1–C2	120.1(4)	C11–C12–C17	127.9(4)
C1–C2–C3	113.6(4)	C13–C12–C17	124.9(4)
C1–C2–C6	121.2(5)	C12–C13–C14	108.4(4)
C3–C2–C6	125.1(5)	C12–C13–C18	123.4(5)
Ru–C3–C2	106.8(3)	C14–C13–C18	127.7(5)
Ru–C3–C4	71.8(2)	C13–C14–C15	107.2(3)
C2–C3–C4	122.7(4)	C13–C14–C19	127.3(4)
Ru–C4–C3	70.7(2)	C15–C14–C19	125.0(4)
Ru–C4–C5	118.3(4)	C11–C15–C14	108.1(3)
C3–C4–C5	121.3(5)	C11–C15–C20	124.0(4)
N–C7–C8	112.4(4)	C14–C15–C20	126.7(4)

the coordinated diene has become converted to a cross-conjugated dienimine ligand, yielding **12**. The shortening of the N–C1 and C2–C6 bonds relative to their diene counterparts (1.274(5) and 1.307(6) Å vs 1.379(8) and 1.507(9) Å) and the lengthening of C1–C2 (1.461(6) vs 1.387(9) Å) also reflect this conversion. As a result, the ruthenium center is now coordinated by a single olefin and the nitrogen lone pair. The Ru–(Cp*) bonding is notably asymmetric, with significantly longer Ru–C bonds for C11 and C12, presumably due to their positioning nearly opposite the coordinated olefin (trans influence). A slight effect of this type was also present opposite to the more strongly bound olefin (C3–C4) in the diene complexes **7**, **8**, and **10**. The Ru–(Cl, N, C3, C4) vectors are all tilted²⁶ relative to the Cp* plane by respective angles of 27.5, 42.5, 24.2, and 45.6°. Thus, there is an alternation in the degree of tilting here, as has been observed in other situations also.²⁷ The binding of the olefin appears enhanced relative to the diene complex, as the Ru–C(3,4) distances are significantly shorter, being ca. 2.170(3) Å. This is reasonable given the incorporation of the better nitrogen donor center into the coordination sphere. The Ru–Cl bond length of 2.447(1) Å is even shorter compared to the correspond-

(26) The sine of the tilt angle was taken to be equal to the additional deviation of a given substituent, relative to Ru, below the Cp* plane, divided by the Ru–substituent bond distance.

(27) (a) Waldman, T. E.; Waltermire, B.; Rheingold, A. L.; Ernst, R. D. *Organometallics* **1993**, *12*, 4161. (b) Waldman, T. E.; Rheingold, A. L.; Ernst, R. D. *J. Organomet. Chem.* **1991**, *401*, 331. (c) Poli, R. *Organometallics* **1990**, *9*, 1892. (d) Lin, Z.; Hall, M. B. *Organometallics* **1993**, *12*, 19.

ing $\text{Cp}^*\text{Ru}(\eta^4\text{-aminodiene})$ complex **2** (2.476(2) Å; vide supra).

Experimental Section

General Procedures. All reactions were performed under a nitrogen atmosphere in reagent grade solvents using Schlenk techniques. THF was distilled from Na/benzophenone, while hexane was distilled from CaH_2 . The ^1H and ^{13}C NMR spectra were recorded on JEOL GSX-270 and JEOL Eclipse-400 spectrometers using deuterated solvents and TMS as an internal reference. Elemental analyses were performed by Robertson Microlit Laboratories, Inc., Madison, NJ. Mass spectra were run on Hewlett-Packard HP-5990A and Finnigan MAT95 (FAB) spectrometers. IR spectra were measured on a Perkin-Elmer/6FPC-FT spectrophotometer using KBr plates for Nujol mulls or a hexane solution cell with NaCl salt plates. Melting points were recorded on compounds in sealed nitrogen-filled capillaries and are uncorrected.

$[\text{Cp}^*\text{RuCl}]_4$ ²⁸ and imines²⁹ were prepared by literature methods. A general method to prepare the organometallic α,β -unsaturated derivatives of group 14 elements is described here, while complete characterization and detailed description of these species will be published elsewhere.¹¹

Synthesis of Imine Derivatives of Silicon, Germanium, and Tin. The appropriate freshly distilled α,β -unsaturated imine (32 mmol) was added to a solution of LDA (32 mmol) in 60 mL of hexane/THF (1:2) at -116°C (EtOH/liquid nitrogen). The reaction mixture was stirred for 7 h and allowed to reach room temperature slowly, after which it was then stirred an additional 1 h. The solution showed a lemon yellow to orange reddish color, depending on the azapentadienide ion. After the reaction mixture was cooled again to -116°C , Me_3MCl (33.6 mmol) in THF (5 mL) was added slowly to the anion. Afterward, the cold bath was removed and the solution was warmed to room temperature, furnishing a colorless solution. The solvent was evaporated, and the white oily residue was extracted with pentane and then filtered from the LiCl. After evaporation of the pentane from the filtrate, the oil was distilled in a horizontal distillation apparatus under reduced pressure (0.05 mmHg). The products distilled between 38 and 71°C , giving yields in the range of 50–82%, the lowest yields being those for tin derivatives.¹¹

Synthesis of $\text{Cp}^*\text{Ru}[\eta^4\text{-CHMe=CHCMe=CHNH}(\text{CMe}_3)]\text{-Cl}$ (2**).** To a THF solution (25 mL) containing 280 mg of $[\text{Cp}^*\text{RuCl}]_4$ (1 mmol) was added 168 mg (1.1 mmol) of $\text{MeCH}_2\text{CH=CH=CMeCH=N}(\text{CMe}_3)$. After it was stirred for 1 h at room temperature, the solution was refluxed for 5 h. The solvent was removed from the red solution in vacuo, and the remaining red-brown residue was redissolved in 40 mL of toluene and the solution filtered through dry Celite. The solution was cooled to -30°C , resulting in the formation of dark red crystals (365 mg, 0.86 mmol, 83% yield), which were decanted and dried under vacuum.

The compound decomposes without melting at $>104^\circ\text{C}$. Anal. Calcd for $\text{C}_{20}\text{H}_{34}\text{NClRu}$: C, 56.54; H, 8.01; N, 3.30. Found: C, 56.25; H, 8.09; N, 3.26. MS (m/e): 425 (2) (M^+), 389 (4), 332 (5), 234 (15), 153 (80), 96 (78), 82 (100), 41 (79).

Synthesis of $\text{Cp}^*\text{Ru}[\eta^4\text{-CH}_2=\text{CHCMe=CHNH}(\text{CMe}_3)]\text{-Cl}$ (3**).** **Method a.** Under a nitrogen atmosphere, $\text{MeCH=CMeCH=N}(\text{CMe}_3)$ (400 mg, 2.9 mmol) was added dropwise to a solution of $[\text{Cp}^*\text{RuCl}]_4$ (217 mg, 0.8 mmol) at room temperature in 25 mL of THF. The reaction mixture was stirred for 1 h at room temperature and then refluxed for 3 h. Filtration and evaporation of the solvent under vacuum gave an oil which was extracted with a mixture of hexane and diethyl ether

(1:1). After the volume of the solvent was reduced and the solution was cooled to -78°C , a red powder precipitated. Filtration afforded 172.5 mg (0.42 mmol, 53%) of **3**.

Synthesis of $\text{Cp}^*\text{Ru}[\eta^4\text{-CH}_2=\text{CHCH=CHNH}(\text{CMe}_3)]\text{-Cl}$ (4**).** **Method a.** This red compound was prepared in the same manner as compound **3**, using the imine $\text{MeCH=CH-CH=N}(\text{CMe}_3)$ (400 mg, 3.2 mmol). The yield was 56% (180 mg, 0.45 mmol).

Method b. Alternatively, under a nitrogen atmosphere, $\text{Me}_3\text{GeCH}_2\text{CH=CHCH=NCMe}_3$ (272 mg, 1.13 mmol) in THF (5 mL) was added dropwise to a cold (-78°C) vigorously stirred solution of $[\text{Cp}^*\text{RuCl}]_4$ (306 mg, 0.281 mmol) in 30 mL of THF. After the solution was warmed to room temperature, stirring was continued for 10 h. The solution was filtered, and the volatiles were removed under vacuum. Compound **4** was then washed with pentane (4×5 mL) at room temperature and extracted with toluene (20 mL). The solvent was evaporated, and the microcrystalline red residue was washed again with pentane (3×5 mL). Recrystallization from a saturated solution of benzene followed by filtration and reduction in vacuo to about 20% of the original volume gave, after freezing and melting of this solution, compound **4** in 68% yield (413 mg, 1.01 mmol).

The compound decomposes without melting at 140°C . MS for $\text{C}_{18}\text{H}_{30}\text{NClRu}$ (m/e): 397 (2) (M^+), 236 (5), 125 (30), 110 (10). IR (cm^{-1}): 1630 (vs), 1605 (vs), 1473 (s), 1452 (s), 1372 (s), 1328 (m), 1308 (m).

Synthesis of $\text{Cp}^*\text{Ru}[\eta^4\text{-HMe=CHCH=CHNH}(\text{CMe}_3)]\text{-Cl}$ (5**) and $\text{Cp}^*\text{Ru}[\eta^5\text{-HMeCHCHCHNH}(\text{CMe}_3)]$ (**6**).** These compounds were prepared by a procedure analogous to that described for **4** (method b) by using a mixture of $\text{Me}_3\text{-SnCHMeCH=CHCH=N}(\text{CMe}_3)$ isomers (650 mg, 2.15 mmol) and $[\text{Cp}^*\text{RuCl}]_4$ (500 mg, 0.46 mmol). After the solution was warmed to room temperature, stirring was continued for 30 min. Compound **6** was extracted from the oily solid with pentane (3×5 mL) at -80°C . The resulting yellow-orange solution was concentrated, and a mass spectrum of the oily residue revealed the expected molecular ion (555 amu). However, all attempts to isolate **6** as a pure compound were unsuccessful. The ^1H NMR spectrum of the mixture showed it to be unstable, giving decomposition products, as well as evidence of the presence of $\text{Cp}^*\text{Ru}[\eta^4\text{-HMeCHCHCHNH}(\text{CMe}_3)]\text{-Cl}$ (**5**), formed as a pentane-insoluble residue. This was washed at room temperature with pentane (3×5 mL) and then extracted with toluene (20 mL). The solvent was evaporated, and the microcrystalline deep red solid was washed again with pentane at room temperature and recrystallized from THF, giving 413 mg (1 mmol, 56%) of **5**. The compound decomposes without melting at 110°C . HRMS for $\text{C}_{19}\text{H}_{32}\text{-NClRu}$: calcd 411.126 68, found 411.1269 (based on ^{102}Ru).

Synthesis of $\text{Cp}^*\text{Ru}[\eta^5\text{-CHMeCHCMeCHN}(\text{CMe}_3)]$ (7**).**

Method a. Under a nitrogen atmosphere, a $n\text{-BuLi}$ (51 mg, 0.5 mL, 1.6 M, 0.8 mmol) solution was added to a cold (-78°C) THF solution (0.50 mL) of diisopropylamine (81 mg, 0.8 mmol). The solution was stirred with slow warming to room temperature. After 15 min the solution was cooled to -78°C and the imine $\text{MeCH}_2\text{CH=CMeCH=N}(\text{CMe}_3)$ (122.4 mg, 0.8 mmol) was added dropwise. After the solution was warmed to room temperature, it was stirred for 1 h. The resulting (azapentadienyl)lithium salt was slowly added dropwise to a cold (-78°C) solution of $[\text{Cp}^*\text{RuCl}]_4$ (217 mg, 0.8 mmol) in 15 mL of THF. After the solution was warmed to room temperature and stirred for 2 h, the volatiles were removed under vacuum. Compound **7** was then extracted from the remaining residue with pentane, and the resulting solution was concentrated and then chromatographed on an Al_2O_3 (grade 1) column (5×1.5 cm) with diethyl ether as the eluant. A yellow band was collected. The solvent was removed in vacuo, and the crude product was recrystallized from hexane at -78°C to give 280 mg (0.72 mmol, 91%) of **7** as a yellow powder.

Method b. Under a nitrogen atmosphere, $\text{Me}_3\text{SnCHMe-}$

(28) (a) Fagan, P. J.; Ward, M. D.; Caspar, J. V.; Calabrese, J. C.; Krusic, P. J. *J. Am. Chem. Soc.* **1989**, *110*, 2981. (b) Fagan, P. J.; Ward, M. D.; Calabrese, J. C. *J. Am. Chem. Soc.* **1989**, *111*, 1698.

(29) (a) Geirsson, J. K. F.; Gudmundsdottir, A. D. *Synthesis* **1990**, 993. (b) Wolf, G.; Wuerthwein, E.-U. *Chem. Ber.* **1991**, *124*, 889.

$\text{CH}=\text{CMeCH}=\text{NCMe}_3$ (574 mg, 1.81 mmol) in THF (5 mL) was added dropwise to a cold (-78°C), vigorously stirred solution of $[\text{Cp}^*\text{RuCl}]_4$ (490 mg, 0.45 mmol) in 30 mL of THF. After the solution was warmed to room temperature, stirring was continued for 30 min. The solution was filtered, and the volatiles were removed under vacuum. Compound **7** was then chromatographed on Florisil with hexane/Et₂O (8:2) as eluent. Yield: 550 mg (1.41 mmol, 78%).

Mp: $116\text{--}118^\circ\text{C}$. Anal. Calcd for $\text{C}_{20}\text{H}_{33}\text{NRu}$: C, 67.82; H, 8.56; N, 3.60. Found: C, 67.85; H, 8.60; N, 3.28. MS (*m/e*): 389 (95) (M^+), 332 (100), 304 (62), 263 (31), 233 (83), 203 (11), 152 (14), 96 (27), 57 (77), 41 (96). IR (cm^{-1}): 2970 (br, vs), 2900 (br, vs), 1510 (m), 1473 (br, vs), 1445 (br, s), 1405 (w), 1368 (vs), 1350 (vs), 1297 (vs), 1265 (vs).

Synthesis of $\text{Cp}^*\text{Ru}[\eta^5\text{-CH}_2\text{CHCMeCHN}(\text{CMe}_3)]$ (**8**).

Method a. This compound was prepared in the same manner as for **7** (method a), using $\text{MeCH}=\text{CMeCH}=\text{N}(\text{CMe}_3)$ (110.7 mg, 0.8 mmol). The yellow, solid product **8** was obtained, in a yield of 95% (284 mg, 0.76 mmol).

Method b. This compound was also prepared in the same manner as for **7** (method b), using $\text{Me}_3\text{SnCH}_2\text{CH}=\text{CMeCH}=\text{N}(\text{CMe}_3)$ (483 mg, 1.6 mmol) and $[\text{Cp}^*\text{RuCl}]_4$ (434 mg, 0.40 mmol). Compound **8** was then chromatographed on alumina with hexane/diethyl ether (9:4), affording 390 mg (1.03 mmol, 65%) of yellow crystals.

Mp: $63\text{--}66^\circ\text{C}$. Anal. Calcd for $\text{C}_{19}\text{H}_{31}\text{NRu}$: C, 60.93; H, 8.34; N, 3.73. Found: C, 59.62; H, 8.44; N, 3.45. MS (*m/e*): 375 (96) (M^+), 316 (100), 315 (69), 290 (63), 263 (26), 233 (65), 203 (6), 165 (2). IR (cm^{-1}): 2970 (br, vs), 2900 (br, vs), 1506 (s), 1470 (br, s), 1458 (br, s), 1448 (br, s), 1406 (m), 1376 (s), 1354 (s), 1276 (vs), 1262 (s).

Synthesis of $\text{Cp}^*\text{Ru}[\eta^5\text{-CH}_2\text{CMeCHCHN}(\text{CMe}_3)]$ (**9**).

Complex **9** was prepared in the same manner as for **7** (method b), using $[\text{Cp}^*\text{RuCl}]_4$ (300 mg, 0.27 mmol) and $\text{Me}_3\text{SnCH}_2\text{-CMe}=\text{CHCH}=\text{N}(\text{CMe}_3)$ (300 mg, 0.27 mmol). Column chromatography was carried out on Florisil using a mixture of hexane and diethyl ether (19:1) as eluent. Yield: 290 mg (0.77 mmol, 71%).

Mp: 48°C . Anal. Calcd for $\text{C}_{19}\text{H}_{31}\text{NRu}$: C, 60.93; H, 8.34; N, 3.73. Found: C, 60.95; H, 8.35; N, 3.29. MS (*m/e*): 375 (79) (M^+), 316 (90), 304 (23), 239 (37), 235 (83), 201 (4), 155 (3). IR (cm^{-1}): 2970 (br, vs), 2900 (br, vs), 1480 (br, vs), 1454 (br, s), 1430 (br, s), 1380 (s), 1354 (s), 1276 (vs).

Synthesis of $\text{Cp}^*\text{Ru}[\eta^5\text{-CH}_2\text{CHCHCHN}(\text{CMe}_3)]$ (**10**).

Method a. This complex was prepared in the same manner as for **7** (method a), using $\text{MeCH}=\text{CHCH}=\text{N}(\text{CMe}_3)$ (99.6 mg, 0.8 mmol). The yellow solid product **10** was obtained, in a yield of 185 mg (0.51 mmol, 75%).

Method b. Complex **10** was also prepared in the same manner as for **7** (method b), using $[\text{Cp}^*\text{RuCl}]_4$ (500 mg, 0.46 mmol) and $\text{Me}_3\text{SnCH}_2\text{CH}=\text{CHCH}=\text{N}(\text{CMe}_3)$ (530 mg, 1.85 mmol). After the volatiles were removed under vacuum, compound **10** was then extracted from the resulting residue with pentane (3×15 mL) at -78°C , affording 490 mg of product (1.36 mmol, 73%). Several sublimations at 50°C and 0.05 mmHg could be used to afford crystals.

Mp: $56\text{--}58^\circ\text{C}$. Anal. Calcd for $\text{C}_{18}\text{H}_{29}\text{NRu}$: C, 59.97; H, 8.10; N, 3.88. Found: C, 59.73; H, 8.17; N, 3.80. MS (*m/e*): 360 (17) (M^+), 361 (27), 346 (12), 306 (5), 304 (9), 235 (23), 233 (25), 178 (2). IR (cm^{-1}): 2970 (br, vs), 2900 (br, vs), 1484 (br, s), 1452 (br, s), 1380 (s), 1354 (s), 1270 (s).

Synthesis of $\text{Cp}^*\text{Ru}[\eta^5\text{-CH}_2\text{CHCHCH}=\text{N}(\text{CMe}_3)](\text{Cl})_2$ (**11**).

This compound was prepared by an analogous procedure as described for **3** (method b), using $\text{Me}_3\text{SiCH}_2\text{CH}=\text{CHCH}=\text{N}(\text{CMe}_3)$ (120 mg, 0.6 mmol) and $[\text{Cp}^*\text{RuCl}]_4$ (160 mg, 0.15 mmol). After the solution was warmed to room temperature, stirring was continued for 15 h. The solid residue was washed with pentane (3×5 mL) at room temperature and then extracted with Et₂O (3×3 mL). A red-brown solid was obtained after evaporation of the ether to dryness. The yield was $\sim 32\%$, but always some impurities were present.

Interconversion Reactions. (a) Compound **10** (20 mg, 0.056 mmol) was dissolved in CDCl_3 (0.5 mL), and the immediate formation of the **11-syn-cis** and **11-syn-trans** isomers was observed by NMR. After 30 min **10** had been completely consumed and the reaction mixture showed **11-syn-cis**, **11-syn-trans**, and **4** in a 6:1:1 ratio. Longer times showed the formation of paramagnetic species and decomposition of the complexes studied.

(b) Compound **10** (20 mg, 0.056 mmol) was dissolved in C_6D_6 (0.5 mL), along with 2 drops of CHCl_3 (CHCl_3 , 1H, δ 6.2). After 3.5 h around 30% of **10** had been consumed and the formation of **11-syn-cis**, a small amount of **11-syn-trans**, traces of **4**, and a compound characterized by an NMR singlet at 6.4 ppm, which is tentatively assigned to $\text{HCIC}=\text{CClH}$ (^1H 6.36 ppm, CCl_4),³⁰ could be observed. After 7.5 h, approximately half of complex **10** had been consumed, and the ratio for **11-syn-cis**, **11-syn-trans**, and **4** was 4:1:1, respectively. Finally, after 20 h, complex **10** had been consumed and the complexes **11-syn-cis**, **11-syn-trans**, and **4** were found in a similar 4:1:1 ratio as before.

(c) Compound **10** (85 mg, 0.236 mmol) was stirred for 15 h at room temperature in 20 mL of C_6H_6 in the presence of a stoichiometric amount of CHCl_3 (18.91 μL). A mixture of complexes **11-syn-cis**, **11-syn-trans**, **4**, and **10** was observed in a ratio of 1:4:1:1.

(d) Compound **10** (100 mg, 0.278 mmol) was dissolved and stirred in CHCl_3 (10 mL) at room temperature. After 20 min the solvent was completely removed and the reaction residue dissolved in C_6D_6 . The ^1H NMR showed the presence of complexes **11-syn-cis** and **11-syn-trans** in a 6:1 ratio, as well as a singlet at 6.4 ppm. Subsequent stirring for 2 h in C_6D_6 afforded a mixture of the respective isomers of compound **11** in a 1.5:1 ratio.

X-ray Structure Determination. Data collection for compounds **2**, **7**, **8**, **10**, and **12** was carried out using an Enraf-Nonius CAD-4 diffractometer. Crystals of **7**, **12**, and **8** were grown at -20°C from hexane and diethyl ether solutions, respectively, while **2** was grown from toluene at -30°C and crystals of **10** were obtained by sublimation. The crystal of compound **7** was mounted on a fiber at room temperature, while that for **8** was mounted in a sealed capillary tube at -70°C for data collection. All structures were solved by direct methods, and all non-hydrogen atoms were subsequently located in Fourier maps and refined anisotropically. Hydrogen atoms on the nitrogen-containing ligand were generally placed in locations derived from difference Fourier maps and, in general, placed in idealized positions. However, for **10**, all hydrogen atoms were positioned in ideal locations and allowed to "ride" with the attached atom. In the case of compound **7** hydrogen atoms were fixed in idealized positions and included in the calculations but not refined themselves, while for compound **8** those hydrogen atoms (H11, H31, H41, H42, H211, H231, H241, and H242) bonded to the azapentadienyl fragment were found in an electron density map and refined isotropically while the remaining hydrogen atoms were fixed in idealized positions and treated as in the case of compound **7**. Calculations for the structures used the MOLEN (**2** and **12**), CRYSTALS (**7** and **8**), or SHELX (**10**) program package. Pertinent bonding parameters are provided in Tables 4–8.

Acknowledgment. Financial support from the National and International Programs supported by CONACYT and NSF is gratefully acknowledged. J.A.G. thanks CONACYT for a research fellowship.

Supporting Information Available: Tables of fractional atomic coordinates, anisotropic thermal parameters, inter-

(30) Standard Spectra, Sadtler Research Lab; Researcher, Editors and Publishers: **1980**, p 6, Spectrum No. 6742.

atomic distances, bond angles, coordinates, interatomic distances, and angles for hydrogen atoms, torsion angles, and least-squares planes for compounds **2**, **7**, **8**, **10**, and **12** and figures giving 1H NMR spectra of compounds **3–6** and **11**. This

material is available free of charge via the Internet at <http://pubs.acs.org>.

OM980875A